Photodermatology, Photoimmunology & Photomedicine

ORIGINAL ARTICLE

Inhibitory effect of 660-nm LED on melanin synthesis in *in vitro* and *in vivo*

Chang Taek Oh[1,2]*, Tae-Rin Kwon[1]*, Eun Ja Choi[1], Soon Re Kim[1], Joon Seok[1], Seog Kyun Mun[3], Kwang Ho Yoo[4], Yeon Shik Choi[5], Sun Young Choi[1] & Beom Joon Kim[1,2]

[1]Department of Dermatology, Chung-Ang University College of Medicine, Seoul, Korea.
[2]Department of Medicine, Graduate School, Chung-Ang University, Seoul, Korea.
[3]Department of Otorhinolaryngology, Chung-Ang University College of Medicine, Seoul, Korea.
[4]Department of Dermatology, College of Medicine, Catholic Kwandong University, International St. Mary's Hospital, Incheon, Korea.
[5]Medical IT Convergence Research Center, Korea Electronics Technology Institute, Gyeonggi-do, Korea.

Key words:
660-nm wavelength; B16F10 cell; HRM-2; light-emitting diode; melanogenesis

Correspondence:
Prof. Beom Joon Kim, M.D., Ph.D., and Prof. Sun Young Choi, M.D., Ph.D., Department of Dermatology, Chung-Ang University Hospital, 102 Heukseokro, Dongjak-gu, Seoul 156-755, Korea.
Tel: +82 2 6299 1525
Fax: +82 2 811 1159
e-mails: beomjoon@unitel.co.kr and sun02ya@naver.com

Accepted for publication:
21 September 2016

Conflicts of interest:
None declared.

*These authors equally contributed as first authors.

SUMMARY

Background
Skin hyperpigmentary disorders including postinflammatory hyperpigmentation, melasma, solar lentigines, and conditions like freckles are common. The light-emitting diodes (LEDs) are the latest category of nonthermal and noninvasive phototherapy to be considered in skin pigmentation disorder treatment.

Purpose
The purpose of this study was to investigate the effects of 660-nm LED on inhibition of melanogenesis. We investigated whether a 660-nm LED affected melanin synthesis in *in vitro* and *in vivo* models, and we explored the mechanisms involved.

Methods
The inhibitory effect of 660-nm LED on melanin synthesis was evaluated in B16F10 cells and HRM-2 melanin-possessing hairless mice were used to evaluate the antimelanogenic effects of 660-nm LED.

Results
Interestingly, 660-nm LED inhibited alpha-melanocyte-stimulating hormone-induced tyrosinase activity in B16F10 cells. We also found that 660-nm LED decreased MITF and tyrosinase expression and induced the activation of ERK. These findings suggest that the depigmenting effects of 660-nm LED result from downregulation of MITF and tyrosinase expression due to increased ERK activity. The 660-nm LED reduced UVB-induced melanogenesis in the skin of HRM-2 via downregulation of tyrosinase and MITF.

Conclusion
These findings suggest 660-nm LED is a potentially depigmentation strategy.

Photodermatol Photoimmunol Photomed 2016; ●●: ●●–●●

doi:10.1111/phpp.12276

Ultraviolet (UV) wavelengths of sunlight are divided into three groups: UVC (200–280 nm), UVB (280–320 nm), and UVA (320–400 nm) (1). UV is a major environmental factor that affects melanogenesis, the essential activity of melanocytes in human skin. UV light exposure can result in hyperpigmentary disorders such as melasma, lentigo, and conditions like freckles (2). Melanin is synthesized by the melanocyte in the basal layer of the epidermis and is stimulated by various factors including alpha-melanocyte-stimulating hormone (α-MSH), UV, and cyclic adenosine monophosphate-elevating agents including isobutylmethylxanthine, forskolin, and glycyrrhizin (3–6). There are three key melanogenic enzymes, tyrosinase, tyrosinase-related protein-1 (TRP-1), and tyrosinase-related protein-2 (TRP-2) (7). The activation or upregulation of melanogenic enzymes increases melanogenesis and pigmentation.

In recent years, phototherapy has been used to treat a broad range of dermatologic conditions. Phototherapy allows the selection of a suitable wavelength from a variety of light energy sources, offering a customizable, efficient, and valuable therapy for a broad range of medical conditions (8, 9). With the recognition of the potential benefits of photobiostimulation (10) and the development and refinement of light-emitting diodes (LEDs), lasers are now used to treat various medical conditions (11). Phototherapy using medical LED devices has been studied during the last decade, recently providing evidence-based results of photobiomodulation (12). A number of clinical studies have provided evidence of the efficacy of LED phototherapy in dermatologic conditions using a variety of LED wavelengths (13). The ideal process of phototherapy should limit thermal damage or photodamage. The useful effects of LED phototherapy have also been reported for applications such as wound healing, anti-inflammation, photorejuvenation, sunburn prevention, resolution of acne vulgaris (14–17). Interestingly, 660-nm LED light has been reported to repair UV-induced skin conditions, such as inflammation and photoaging, suggesting that the mechanisms of action for 660-nm LED and UV radiation are different (18). However, the inhibitory effect of 660-nm LED on melanogenesis has been established in the literature (19).

Therefore, we examined whether 660-nm LED affected melanogenesis. In order to understand the mechanism and evaluate the benefits of 660-nm LED phototherapy, we evaluated α-MSH-induced melanogenesis in B16F10 cells. We also evaluated an *in vivo* model of UVB-induced hyperpigmentation using melanin-possessing hairless mice.

MATERIALS AND METHODS

Light sources and irradiation

The LED device used (Korea Electronics Technology Institute, Gyeonggi-do, Korea) produced light at a wavelength of 660 nm. To minimize heat generation, the LED arrays were equipped with electric cooling systems at the back of the arrayed lamps. All cell cultures were irradiated with a 660-nm LED (7.8 mJ/cm^2). To avoid absorption by the colored culture media, the cells were washed twice with phosphate-buffered saline and irradiated 5 cm from the LED device (20).

Reagents

α-MSH, 3,4-dihydroxy-L-phenylalanine (L-DOPA), and PD98059 were purchased from Sigma-Aldrich Co. (St. Louis, MO, USA). Cell Counting Kit-8 (CCK-8) was purchased from Dojindo Molecular Technologies, Inc. (Kumamoto, Japan). Dulbecco's modified Eagle's medium (DMEM), trypsin–ethylenediaminetetraacetic acid (EDTA), DPBS, and penicillin/streptomycin were purchased from Welgene Biopharmaceuticals (Daegu, Korea). Fetal bovine serum (FBS) was purchased from Life Technologies Co. (Gibco, Life Technologies, NY, USA). Antibodies specific for phospho-ERK1/2 (Thr202/Tyr204, #9101), ERK1/2 (#9102), phospho-p38 MAPK (Thr180/Tyr182, #4511), p38 MAPK (#9212), phospho-JNK (Thr183/Tyr185, #9251), JNK (#9252), and β-actin (#4967) were purchased from Cell Signaling Technology (Beverly, MA, USA). Antibodies specific for tyrosinase (M-19, sc-7834), TRP-1 (H-90, sc-25543), and TRP-2 (H-150, sc-25544) were purchased from Santa Cruz Biotechnology, Inc. (Santa Cruz, CA, USA). MITF Ab-1 (C5, MS-771-P0) was purchased from Thermo Scientific (Fremont, CA, USA). Secondary antibodies for anti-goat IgG (PI-9500), anti-mouse IgG (PI-2000), and anti-rabbit IgG (PI-1000) were purchased from Vector Laboratories (Burlingame, CA, USA).

Cell culture

B16F10 cells (CRL-6475) were purchased from the American Type Culture Collection (Rockville, MD, USA). Cells were cultured in DMEM supplemented with 10% FBS and 1% penicillin/streptomycin (Welgene, Daegu, Korea) and incubated at 37°C in a humidified atmosphere of 5% CO_2.

Cell viability assay

The viability of irradiated cells was established using CCK-8, as explained by the manufacturer. The cells were irradiated with 660-nm LED at different intensity values. After 24 h, the media containing irradiated cells were replaced with media containing 10% CCK-8 solution. Cells were then incubated at 37°C for 30 min, and the absorbance was measured at 450 nm using a spectrophotometer (VersaMax; Molecular Devices, CA, USA).

Measurement of melanin content

The cells were irradiated with 660-nm LED at 2.5–10 J/cm^2 and then incubated in phenol red-free DMEM for 10% FBS for 72 h. The optical density of each supernatant media was measured at 405 nm using a spectrophotometer.

Tyrosinase activity assay

Tyrosinase activity in B16F10 cells was determined using a literature method with slight modification (21). The cells were irradiated with 660-nm LED at 2.5–10 J/cm^2 and then incubated in DMEM for 10% FBS for 72 h. The cells were lysed in 150 μl of phosphate buffer (0.1 M), pH 6.8, containing 1% Triton X-100. The cellular extract was clarified by centrifugation at 3000 g for 10 min. After the quantification of protein level and the adjustment of concentration using lysis buffer, each extract (180 μl) was added to a 96-well plate, and the enzymatic assay was initiated by adding 20 μl of $_L$-DOPA solution at 37°C. The absorbance at 475 nm and 37°C was read every 10 min for at least 30 min using a spectrophotometer.

Western blot analysis

Protein extracts were lysed using cold RIPA buffer (50 mM Tris–HCl, pH 7.2, 150 mM NaCl, 1% NP40, 0.1% SDS, 0.5% DOC, 1 mM PMSF, 25 mM MgCl2, and phosphatase inhibitor cocktail). The amount of protein in cell extracts was quantified using a BCA Protein Assay kit. Equal amounts of protein per well were resolved on 10% SDS-PAGE and blotted onto PVDF membranes (Millipore, Billerica, MA, USA), which were then blocked with 5% skim milk in Tris-buffered saline containing 0.5% Tween-20 (Sigma-Aldrich Co., St. Louis, MO, USA). The membrane was probed with specific antibodies and incubated with HRP-conjugated secondary antibodies. Antibodies were detected using enhanced chemiluminescence reagents (Amersham Pharmacia, Piscataway, UK).

Immunocytochemistry

The cells were fixed with 4% paraformaldehyde for 15 min at room temperature. The cells were treated with 0.01% Triton X-100 in PBS for 15 min at room temperature and then blocked with 2% bovine serum albumin in PBS for 60 min at room temperature. The slides were incubated overnight with tyrosinase antibodies (ab180753, Abcam) at 4°C. The slides were incubated with FITC-conjugated goat anti-rabbit IgG (1 : 1000, NB730-F, Novus Biologicals, CO, USA) and mounted using DAPI (Golden Bridge International, Inc., WA, USA).

UVB-induced hyperpigmentation in HRM-2

Six-week-old male HRM-2 melanin-possessing hairless mice (total = 24) were obtained from Hoshino Laboratory Animals (Saitama, Japan) and housed in an air-conditioned room maintained at 24°C ± 2°C and 55% ± 15% humidity with a 12-h light–dark cycle. All procedures involving animals were conducted in accordance with the guidelines of the Institutional Animal Care and Use Committee of Chung-Ang University in Korea (IACUC Number: 14-0054). Mice were randomly divided into four groups (n = 6 per group. The mice were anesthetized with Zoletil 50 (50 mg/kg) and xylazine (10 mg/kg). The dorsal skin of each mouse was irradiated with 660-nm LED before UVB exposure (BIO-SPECTRA; Vilber Lourmat, France). The experimental schedule is detailed in Fig. 5a. The color of each skin site was measured using a spectrophotometer (CR-10; Konica Minolta Sensing Inc., Osaka, Japan).

Histopathological analysis

Dorsal skin samples were fixed in 4% paraformaldehyde, embedded in paraffin, and sliced into 5-μm sections. Skin sections were stained with H&E and Fontana–Masson for melanin. Additional skin sections were stained for immunohistochemical markers using monoclonal antibodies against tyrosinase (1 : 500, ab180753, Abcam), MITF (1 : 200, NBP1-61363, Novus), and Melan-A (1 : 200, NBP1-30151, Novus).

Statistical analysis

All data analysis was performed at least three times, and the results are expressed as mean ± standard deviation.

The data were analyzed using one-way ANOVA (SPSS software, SPSS Inc., Chicago, IL, USA). Values of $P < 0.05$ (*), $P < 0.01$ (**), and $P < 0.001$ (***) were considered significantly different.

RESULTS

Effect of 660-nm LED on the melanogenesis of B16F10 cells

To investigate whether 660-nm LED has cell viability on cells, we irradiated LED range of 0–20 J/cm^2. As shown in Fig. 1a, 660-nm LED treatment reduced cell viability to less than 20% ($P = 0.001929$) at 15 J/cm^2. To determine whether 660-nm LED inhibited melanin synthesis, we measured the melanin content of B16F10 cells. We used PTU as a positive control in these experiments because PTU has known inhibitory effects on melanin synthesis. Melanin contents were significantly reduced in a dose-dependent manner by 660-nm LED irradiation in B16F10 cells (Fig. 1b). In addition, 660-nm LED at the same dose also decreased tyrosinase activity in B16F10 cells (Fig. 1c).

Effect of 660-nm LED on the expression levels of proteins related to melanogenesis

To determine whether the effect of 660-nm LED light was related to melanogenesis, we evaluated expression in tyrosinase, TRP-1, TRP-2, and MITF protein levels in a day-course experiment 24–72 h after the cells were irradiated with 660-nm LED at 10 J/cm^2 and prior to stimulation in the presence of α-MSH (Fig. 2a). Furthermore, the effect of 660-nm LED on tyrosinase expression level was assessed through immunocytochemistry (Fig. 2b). The results showed that the level of

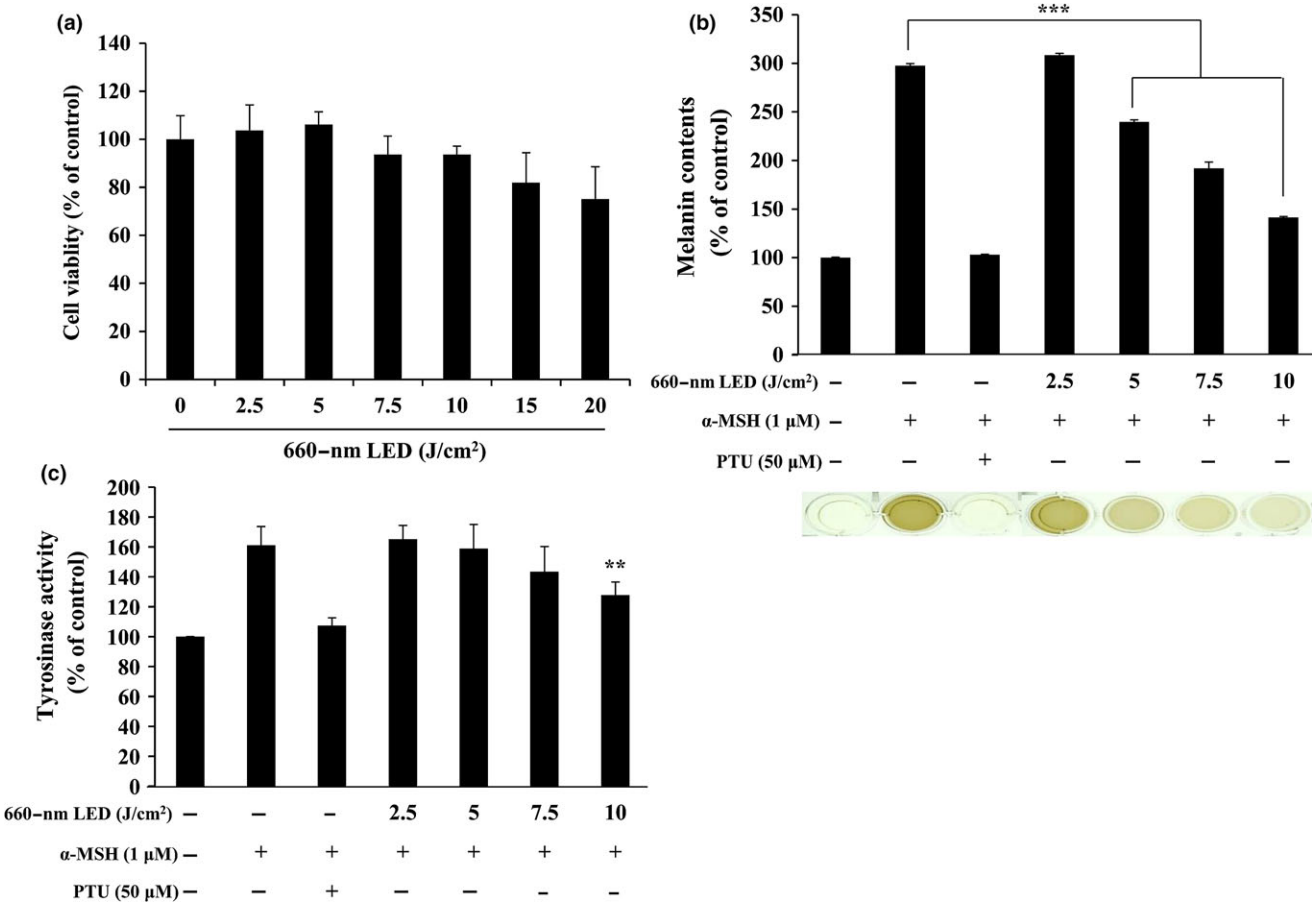

Fig. 1. Effect of 660-nm light-emitting diode (LED) on melanogenesis of B16F10 cells. (a) Cell viability was then measured using CCK-8 assays. Each result represents the mean ± SD of triplicate experiments. (b) and (c) The cells were irradiated with 660-nm LED at 2.5–10 J/cm^2 in the presence of α-melanocyte-stimulating hormone (α-MSH: 1 μM) for 72 h. 50 μM phenylthiourea (PTU) was used as the positive control. Melanin content (b) and tyrosinase activity (c) were measured as described in the Materials and Methods. Each result represents the mean ± SD of triplicate experiments. **$P < 0.01$, ***$P < 0.005$ compared with α-MSH-treated controls (b and c).

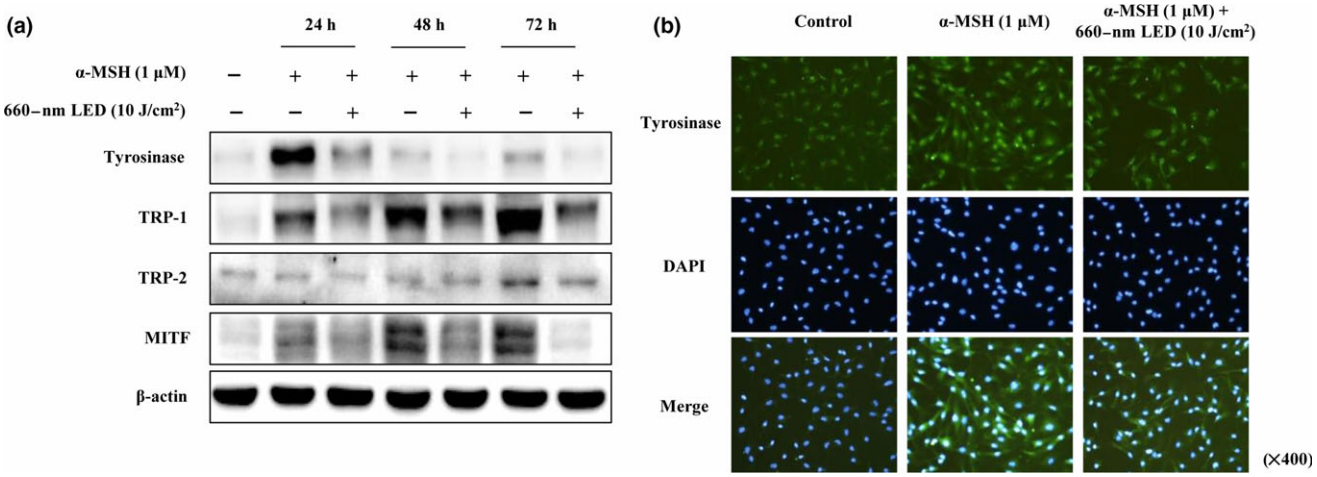

Fig. 2. Effect of 660-nm light-emitting diode on the expression of proteins related to melanin synthesis. (a) Whole-cell lysates were analyzed by Western blot analysis with antibodies against tyrosinase, tyrosinase-related protein-1 (TRP-1), tyrosinase-related protein-2 (TRP-2), and microphthalmia-associated transcription factor (MITF). Equal protein loadings were verified using β-actin antibodies. (b) Tyrosinase was evaluated by immunofluorescence staining using specific tyrosinase antibodies (green). Corresponding 4,6-diamino-2-phenylindole (DAPI) nuclear staining (blue) and merged images are shown. Fluorescence was detected under a fluorescence microscope. The specimens were photographed using DP Controller software (×400 magnification).

tyrosinase expression in cells was decreased by 660-nm LED after 72 h in the presence of α-MSH.

Effect of 660-nm LED on ERK phosphorylation in B16F10 cells

To elucidate the mechanisms underlying the inhibitory effect of 660-nm LED on melanogenesis, we characterized the changes in melanogenesis-related signals using Western blot analysis in a time-course experiment. Because the phosphorylation of ERK has been reported to trigger MITF degradation, we examined whether 660-nm LED influenced ERK activation. As shown in Fig. 3a, the phosphorylation of ERK in B16F10 cells was induced by 660-nm LED at 120 min after irradiation. Because the phosphorylation of ERK has been reported to decrease melanin synthesis, we confirmed whether the 660-nm LED-induced phosphorylated ERK signaling pathways were involved in cellular melanin synthesis in B16F10 cells irradiated with 660-nm LED for 30 min in the presence or absence of PD98059 (ERK inhibitor). As shown in Fig. 3b, the melanin contents in B16F10 cells co-cultured with α-MSH and PD98059 were higher than those in cells cultured with α-MSH alone. Additionally, these synergistic effects of α-MSH and PD98059 on melanin contents were offset by 660-nm LED irradiation. We evaluated whether PD98059 inhibits phosphorylation of the ERK pathway in B16F10 cells and found that PD98059 does block ERK phosphorylation (Fig. 3c).

Effect of 660-nm LED on UVB-induced melanogenesis in HRM-2

The effects of 660-nm LED on melanogenesis were evaluated in HRM-2 mice. The dorsal skin color of HRM-2 mice was photographed using a digital camera (5200D; Canon Inc., Tokyo, Japan). These results showed that 660-nm LED is effective at decreasing melanin synthesis in a UVB-induced hyperpigmentation (Fig. 4b). The mice were irradiated with or without 660-nm LED and repeated UVB irradiation led to melanogenesis. The color of the dorsal skin areas was measured using a CR-10 spectrophotometer. We observed a dose-dependent increase in *L*-value of 660-nm LED-irradiated mice compared to UVB-irradiated group. Total *L*-value changes were calculated by subtracting first day *L*-values from last day *L*-values. The 660-nm LED-irradiated groups showed a significant inhibition effect compared to UVB-irradiated group (Fig. 4c).

Effect of 660-nm LED on UVB-induced histopathological analysis in HRM-2

H&E-stained dorsal skin tissues were obtained after 17 days, and the status of the epidermis was observed using optical microscopy. 660-nm LED had inhibitory effects on UVB-induced epidermal and dermal condition (Fig. 5a) and significantly decreased epidermis thickness compared to UVB-irradiated group (Fig. 5b). These results indicate that 660-nm LED protects UVB-induced

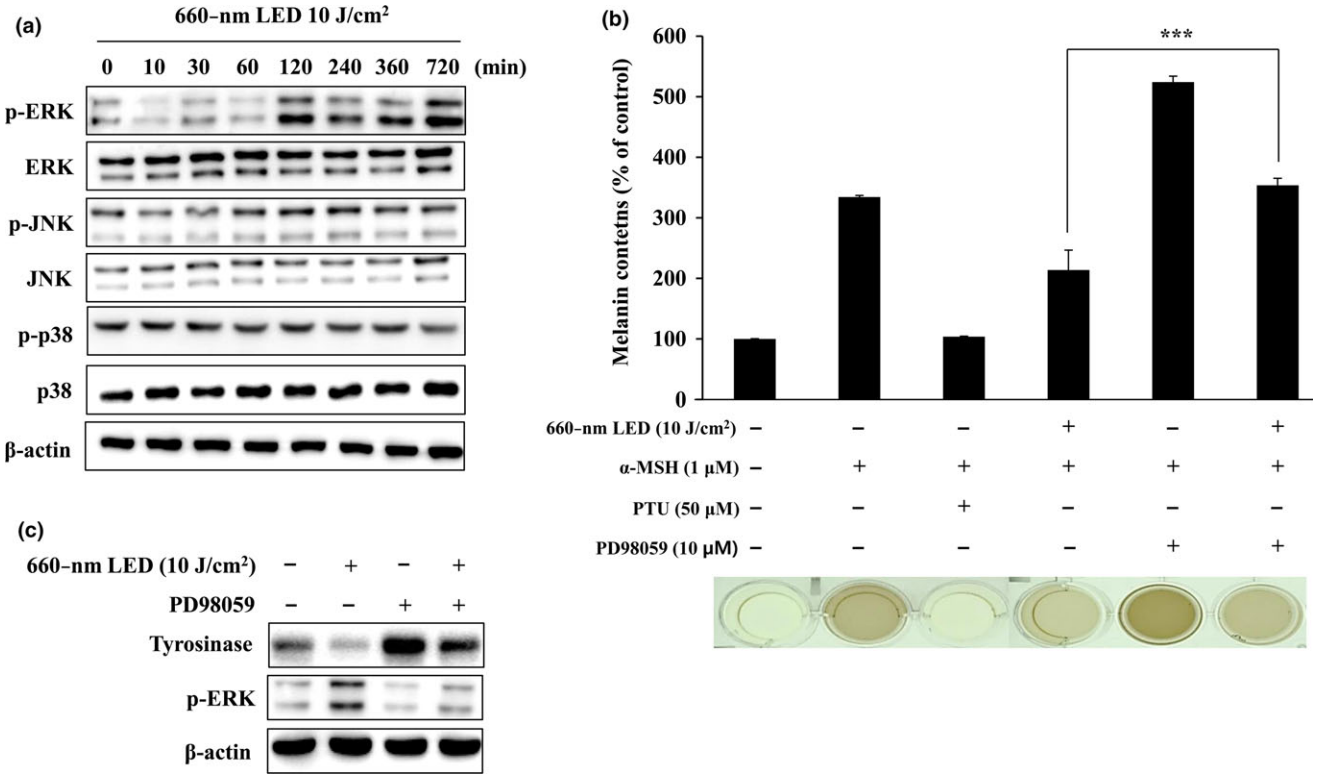

Fig. 3. Effect of 660-nm light-emitting diode (LED) on ERK phosphorylation in B16F10 cells. (a) Western blot analysis using antibodies against phospho-specific ERK (p-ERK), phospho-specific JNK (p-JNK), and phospho-specific p38 (p-p38). Equal protein loading was verified using β-actin, phosphorylation-independent ERK, JNK, and p38 antibodies. (b) The cells were pretreated with 20 μM of PD98059 for 30 min and then irradiated with 660-nm LED at 10 J/cm2 and cultured for 72 h. 50 μM phenylthiourea (PTU) was used as the positive control. Melanin content was measured as described in the Materials and Methods. Each result represents the mean ± SD of triplicate experiments. ***$P < 0.005$ compared with the 660-nm LED-irradiated group. (c) Whole-cell lysates were prepared and subjected to Western blot analysis using antibodies against tyrosinase and phospho-specific ERK. Equal protein loadings were verified using β-actin antibodies.

hyperkeratosis. To visualize melanin contents of basal layer of epidermis, dorsal skin tissue was stained with Fontana–Masson stain and observed. As shown in Fig. 5c, 660-nm LED groups had significant and dose-dependent decreases compared with the UVB-irradiated group. In addition, we performed immunohistochemistry to confirm the expression changes in dorsal skin tissue protein expression using the melanogenesis markers S100, Melan-A, tyrosinase, and MITF antibodies. 660-nm LED light-irradiated group demonstrated significant and dose-dependent decreases in protein expression compared with the UVB-irradiated group.

DISCUSSION

Melanogenesis is the major protective mechanism against sun-related injuries in human skin and is responsible for skin color (22). Unusual synthesis of melanin in melanocytes is responsible for pigmented skin disorders such as hyperpigmentation, melasma, and senile lentigines and skin conditions like freckles after UV exposure (23). A large number of medical devices, lasers, and chemical and biological agents have been developed. Only a few of these efforts have demonstrated therapeutic efficacy and clinical utility, mostly due to unwanted side effects and cytotoxicity. Therefore, it is necessary to better understand the fundamental mechanism behind pigmentation and to develop safer, more effective treatment devices and agents.

We examined whether 660-nm LED represents an effective depigmentation treatment. We confirmed no cytotoxicity in an intensity range from 2.5 to 10 J/cm^2 (Fig. 1a). In addition, melanin contents were significantly decreased in a dose dependently with 660-nm LED from 5 to 10 J/cm^2 (Fig. 1b). These results suggest that 660-nm LED inhibits melanin synthesis. For a better understanding of the inhibitory effect of 660-nm LED on tyrosinase, we confirmed that tyrosinase, TPR-1, TPR-2, and MITF protein expression were decreased by 660-nm LED in a day-dependent manner (Fig. 2a) and

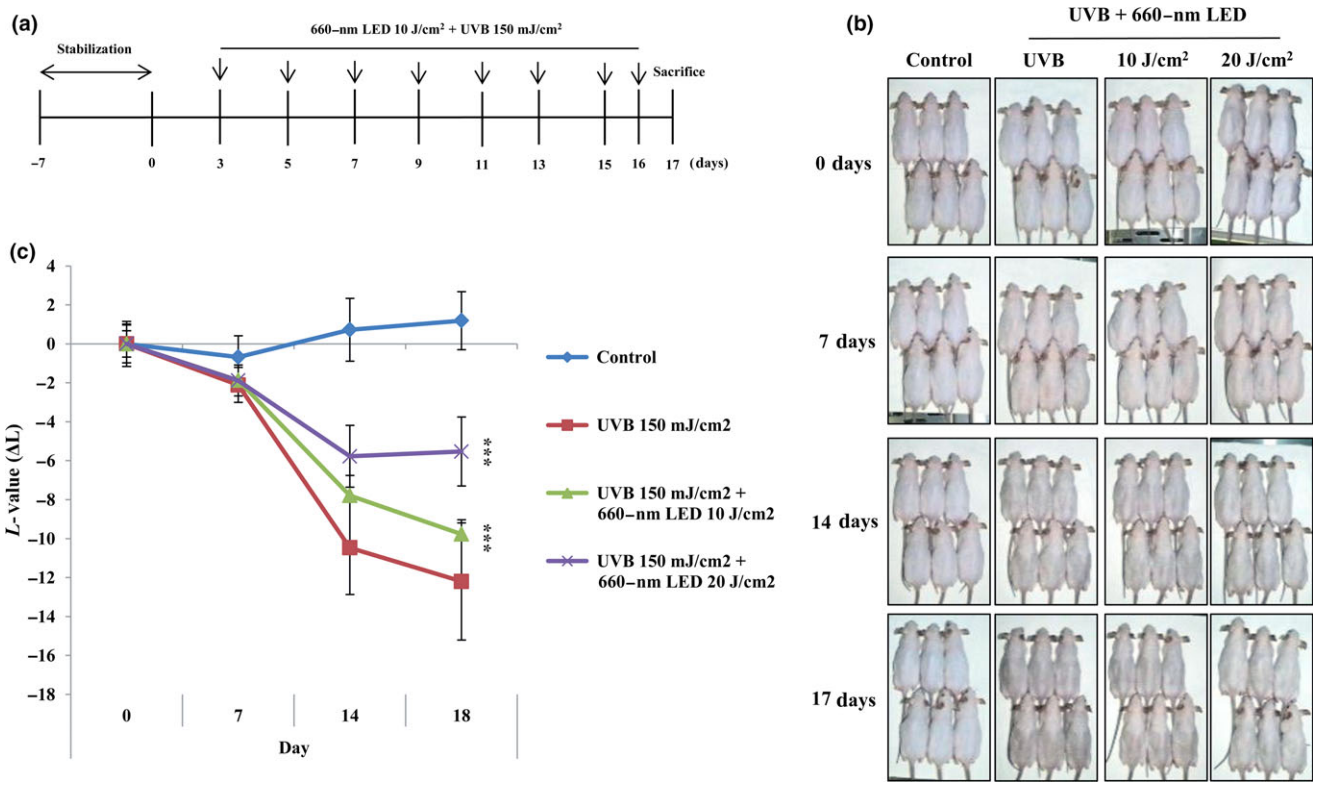

Fig. 4. Effect of 660-nm light-emitting diodes (LED) on UVB-induced hyperpigmentation in HRM-2. (a) Experimental schedule design. HRM-2 mice were irradiated with 660-nm LED light (10 and 20 J/cm^2) and exposed to UVB (150 mJ/cm^2) at the indicated times (arrow). (b) Representative photographs showing the lightening effects of 660-nm LED light on UVB-induced melanogenesis. All photographs are from the same groups. (c) For statistical analysis, change in *L*-value of each animal was calculated as average values of the dorsal skin of HRM-2 mice. The ΔL-value before and 17 days after irradiation with 660-nm LED and UVB was measured using a CR-10 chromameter. Groups of six animals were used in this experiment. Each result represents the mean ± SD of ΔL-value. ***$P < 0.005$ compared with the UVB-irradiated group.

660-nm LED-induced depigmentation was associated with decreased tyrosinase activity (Fig. 1c). In addition, the effect of 660-nm LED on tyrosinase expression was confirmed by immunofluorescence (Fig. 2b). These results indicate that 660-nm LED inhibits the expression levels of tyrosinase, TRP-1, TRP-2, and MITF, which play regulatory roles in melanogenesis at translational and transcriptional expression.

To investigate the mechanism underlying the depigmentation effect of 660-nm LED, changes in melanogenesis-related transduction pathways induced by 660-nm LED were confirmed by Western blot analysis in a time-course experiment (Fig. 3a). It has been reported that ERK is a significant regulator of melanogenesis because phosphorylated ERK induces MITF phosphorylation and degradation and thus reduces melanin synthesis (24). Previous studies have demonstrated that phosphorylated ERK is related to cAMP-induced melanogenesis (25). However, previous studies have also confirmed that constitutive mutants of Ras and MEK suppress tyrosinase transcription (26). Phosphorylated ERK is known to phosphorylate MITF at serine 409. In addition, phosphorylated MITF has been reported to be a marker of proteolysis through the ubiquitin-dependent proteasome pathway (27). We evaluated a specific ERK inhibitor, PD98059, and confirmed that 660-nm LED-induced depigmentation was restored by PD98059 treatment (Fig. 3b). We also showed that 660-nm LED phosphorylated ERK and inhibited tyrosinase protein expression. To our knowledge, this is the first demonstration of the phosphorylation of ERK by 660-nm LED. To examine the relationship between ERK phosphorylation and tyrosinase downregulation, we pretreated cells with PD98059 before 660-nm LED irradiation, re-evaluated phosphorylation ERK protein expression level, and confirmed that ERK phosphorylation inhibited melanogenesis (Fig. 3c).

The inhibitory effects of 660-nm LED on melanogenesis were also evaluated using a HRM-2 mice model, which is the typical animal model in this type of study

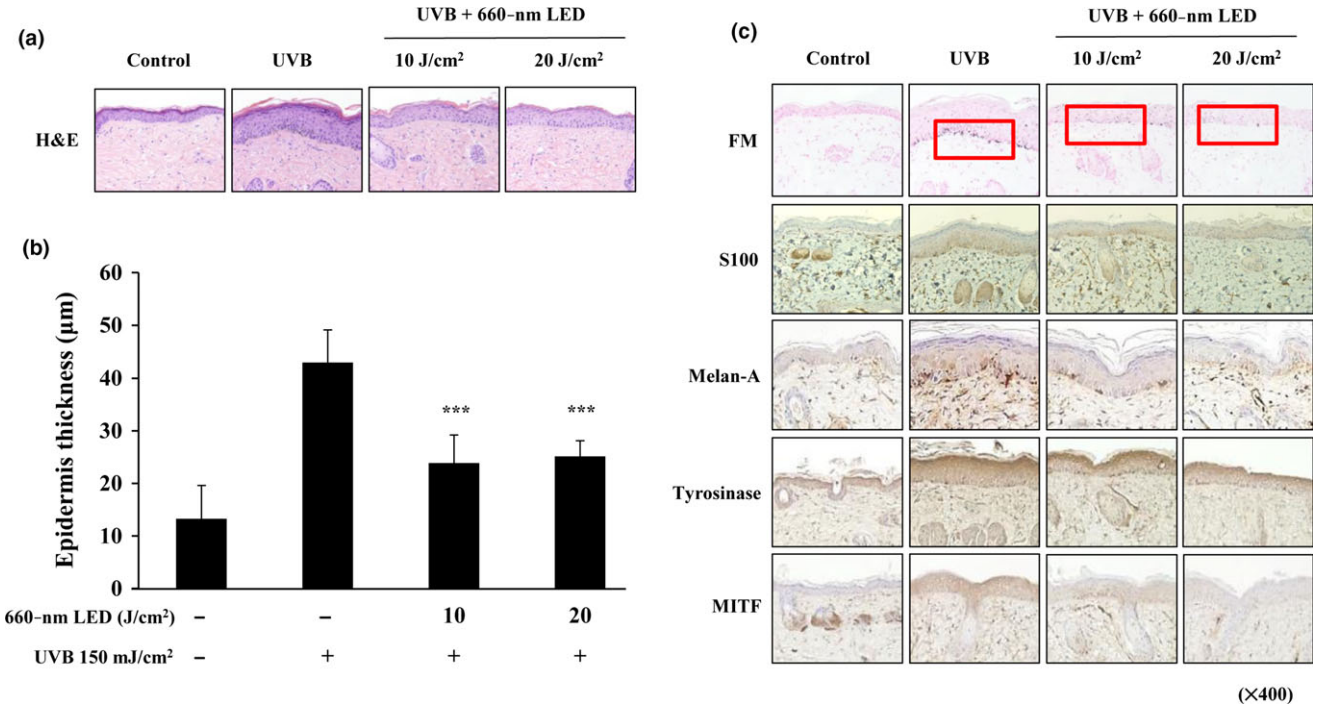

Fig. 5. Effect of 660-nm light-emitting diodes (LED) on UVB-induced histopathology in HRM-2. (a) Tissue morphology of UVB-induced skin tissue stained with hematoxylin–eosin (H&E). (b) Epidermal thickness of dorsal skin was measured under an optical microscope. Each result represents the mean ± SD of epidermis thickness (n = 6). ***P < 0.005 compared with the UVB-irradiated group. (c) Melanin is stained black with Fontana and Masson stain (FM). Sections immunohistochemically stained with S100, Melan-A, tyrosinase, and MITF antibodies are shown. Sections were stained with diaminobenzidine (DAB) and hematoxylin counterstain for visualization of nuclei. Brown dots signify positively stained cells. The images are representative examples from each group (×400 magnification).

(28). In this model, 660-nm LED showed a significant inhibitory effect on UVB-induced melanogenesis (Fig. 4b,c). These results suggest that the depigmentation effect of 660-nm LED on UVB-induced melanogenesis acts through prevention of melanin synthesis in active melanocytes. We also evaluated the dorsal skin of HRM-2 mice using H&E and Fontana–Masson stains in order to characterize skin condition and melanin contents. As shown in Fig. 5, we confirmed that 660-nm LED significantly decreased epidermis thickness and reduced melanin contents in a dose-dependent manner. To better understanding the depigmentation mechanism, we investigated the expression levels of S100, Melan-A, tyrosinase, and MITF using an immunohistochemistry assay. Tyrosinase and MITF regulate significant biological effects in the skin including pigmentation, dendrite formation, and melanocyte proliferation. Furthermore, S100 and Melan-A demonstrate pigmentation status in the epidermis or epidermis basal layer (29). The 660-nm LED decreased the protein levels of S100, Melan-A, tyrosinase, and MITF. These results demonstrate the inhibitory effect of 660-nm LED on UVB-induced hyperpigmentation.

In conclusion, the 660-nm LED might prove to be a useful therapy for treating patients with hyperpigmentation. However, further studies, including clinical studies and efficiency and safety evaluations, are required to confirm these effects because of our results performed B16F10 melanoma cells not human. So we should perform study on mechanism in human.

ACKNOWLEDGEMENTS

This work was supported by the Infrastructure Program for New Growth Industries (10044186, Development of Smart Beauty Devices Technology and Establishment of Commercialization Support Center) funded by the Ministry of Trade, Industry & Energy (MI, Korea).

REFERENCES

1. Nole G, Johnson AW. An analysis of cumulative lifetime solar ultraviolet radiation exposure and the benefits of daily sun protection. *Dermatol Ther* 2004; **17**(Suppl. 1): 57–62.
2. Hearing VJ. Determination of melanin synthetic pathways. *J Invest Dermatol* 2011; **131**: E8–E11.
3. Chakraborty A, Slominski A, Ermak G, Hwang J, Pawelek J. Ultraviolet B and melanocyte-stimulating hormone (MSH) stimulate mRNA production for alpha MSH receptors and proopiomelanocortin-derived peptides in mouse melanoma cells and transformed keratinocytes. *J Invest Dermatol* 1995; **105**: 655–659.
4. Chakraborty AK, Funasaka Y, Slominski A *et al.* UV light and MSH receptors. *Ann N Y Acad Sci* 1999; **885**: 100–116.
5. Kadekaro AL, Kanto H, Kavanagh R, Abdel-Malek Z. Significance of the melanocortin 1 receptor in regulating human melanocyte pigmentation, proliferation, and survival. *Ann N Y Acad Sci* 2003; **994**: 359–365.
6. Oh CT, Lee D, Koo K *et al.* Superoxide dismutase 1 inhibits alpha-melanocyte stimulating hormone and ultraviolet B-induced melanogenesis in murine skin. *Ann Dermatol* 2014; **26**: 681–687.
7. Hirobe T. Role of keratinocyte-derived factors involved in regulating the proliferation and differentiation of mammalian epidermal melanocytes. *Pigment Cell Res* 2005; **18**: 2–12.
8. Opel DR, Hagstrom E, Pace AK *et al.* Light-emitting diodes: a brief review and clinical experience. *J Clin Aesthet Dermatol* 2015; **8**: 36–44.
9. Lim HW, Silpa-archa N, Amadi U, Menter A, Van Voorhees AS, Lebwohl M. Phototherapy in dermatology: a call for action. *J Am Acad Dermatol* 2015; **72**: 1078–1080.
10. Nadur-Andrade N, Barbosa AM, Carlos FP, Lima CJ, Cogo JC, Zamuner SR. Effects of photobiostimulation on edema and hemorrhage induced by Bothrops moojeni venom. *Lasers Med Sci* 2012; **27**: 65–70.
11. Bucci J, Goldberg D. Past, present, and future: vascular lasers/light devices. *J Cosmet Laser Ther* 2006; **8**: 149–153.
12. Wunsch A, Matuschka K. A controlled trial to determine the efficacy of red and near-infrared light treatment in patient satisfaction, reduction of fine lines, wrinkles, skin roughness, and intradermal collagen density increase. *Photomed Laser Surg* 2014; **32**: 93–100.
13. Tsibadze A, Chikvaidze E, Katsitadze A, Kvachadze I, Tskhvediani N, Chikviladze A. Visible light and human skin (Review). *Georgian Med News* 2015; **246**: 46–53.
14. de Vasconcelos Catao MH, Nonaka CF, de Albuquerque RL Jr, Bento PM, de Oliveira Costa R. Effects of red laser, infrared, photodynamic therapy, and green LED on the healing process of third-degree burns: clinical and histological study in rats. *Lasers Med Sci* 2015; **30**: 421–428.
15. Kim CH, Cheong KA, Lee AY. 850 nm light-emitting-diode phototherapy plus low-dose tacrolimus (FK-506) as combination therapy in the treatment of dermatophagoides farinae-induced atopic dermatitis-like skin lesions in NC/Nga mice. *J Dermatol Sci* 2013; **72**: 142–148.
16. Ko DY, Jeon SY, Kim KH, Song KH. Fractional erbium: YAG laser-assisted photodynamic therapy for facial actinic keratoses: a randomized, comparative, prospective study. *J Eur Acad Dermatol Venereol* 2014; **28**: 1529–1539.
17. Lambrecht P, Vandeplas G, Van Slycke S, Smet PF, Brusselaers N, Vermeersch H. Phototoxic reaction after parathyroid surgery: case report and review of the literature. *Acta Clin Belg* 2012; **67**: 438–441.
18. Barolet D, Roberge CJ, Auger FA, Boucher A, Germain L. Regulation of skin collagen metabolism *in vitro* using a pulsed 660 nm LED light source: clinical correlation with a single-blinded study. *J Invest Dermatol* 2009; **129**: 2751–2759.
19. Barolet D, Boucher A. LED photoprevention: reduced MED response following multiple LED exposures. *Lasers Surg Med* 2008; **40**: 106–112.
20. Babilas P, Kohl E, Maisch T *et al. In vitro* and *in vivo* comparison of two different light sources for topical photodynamic therapy. *Br J Dermatol* 2006; **154**: 712–718.
21. Kim JH, Baek SH, Kim DH *et al.* Downregulation of melanin synthesis by haginin A and its application to *in vivo* lightening model. *J Invest Dermatol* 2008; **128**: 1227–1235.
22. Riley PA. Melanins and melanogenesis. *Pathobiol Annu* 1980; **10**: 223–251.
23. Holzle E. Pigmented lesions as a sign of photodamage. *Br J Dermatol* 1992; **127** (Suppl 41): 48–50.
24. Wu M, Hemesath TJ, Takemoto CM *et al.* c-Kit triggers dual phosphorylations, which couple activation and degradation of the essential melanocyte factor Mi. *Genes Dev* 2000; **14**: 301–312.
25. Englaro W, Rezzonico R, Durand-Clement M, Lallemand D, Ortonne JP, Ballotti R. Mitogen-activated protein kinase pathway and AP-1 are activated during cAMP-induced melanogenesis in B-16 melanoma cells. *J Biol Chem* 1995; **270**: 24315–24320.
26. Kahn V. Effect of kojic acid on the oxidation of DL-DOPA, norepinephrine, and dopamine by mushroom tyrosinase. *Pigment Cell Res* 1995; **8**: 234–240.
27. Xu W, Gong L, Haddad MM *et al.* Regulation of microphthalmia-associated transcription factor MITF protein levels by association with the ubiquitin-conjugating enzyme hUBC9. *Exp Cell Res* 2000; **255**: 135–143.
28. Yun CY, You ST, Kim JH *et al.* p21-activated kinase 4 critically regulates melanogenesis via activation of the CREB/MITF and beta-catenin/MITF pathways. *J Invest Dermatol* 2015; **135**: 1385–1394.
29. Viray H, Bradley WR, Schalper KA, Rimm DL, Gould Rothberg BE. Marginal and joint distributions of S100, HMB-45, and Melan-A across a large series of cutaneous melanomas. *Arch Pathol Lab Med* 2013; **137**: 1063–1073.